Mechanisms Controlling Release of Colloids to Groundwater in a Southeastern Coastal Plain Aquifer Sand

CHRISTOPHER H. SWARTZ AND
PHILIP M. GSCHWEND*

Ralph M. Parsons Lab, 48-415, Massachusetts Institute of Technology, 15 Vassar Street, Cambridge, Massachusetts 02139

The release of colloids from a shallow Southeastern Coastal Plain deposit, in response to treatment with solutions that perturbed electrostatic and cementitious associations among the clay-size constituents, suggested that these constituents are predominantly chemically bound within the interstitial matrix. Sediment-packed columns subjected to a sequence of high/low ionic strength solutions, acidic pH (2.6) solutions, and anionic surfactant solutions yielded undetectable colloid releases. Treatment with elevated pH (8.8) solutions and solutions containing phosphate resulted in mobilization of colloids only partially representative of the bulk matrix. Organic acids, which both (i) initiated dissolution of the amorphous iron oxyhydroxide intermediaries among kaolinite books and (ii) imparted negative charge to the iron oxyhydroxide surfaces to generate sufficiently repulsive forces among the juxtaposed matrix constituents, appeared to induce mobilization of colloids compositionally representative of the entire bulk matrix. These results suggest that "cross-bonding" of juxtaposed matrix constituents in this sediment may hinder colloid mobilization in response to only electrostatic perturbations, an effect that must be considered to accurately predict colloid mobilization and concomitant facilitated transport in this and other diagenetically similar deposits.

Introduction

The potential for colloid migration to facilitate the subsurface transport of contaminants motivates research focused on understanding the properties and generation of groundwater colloids (*1−3*). Predominantly inorganic phases (e.g., clay minerals; iron, manganese, and aluminum oxides; and quartz) have been implicated as colloidal phases in field observations of groundwater colloids (*4−6*). Inorganic colloids are generated by a variety of mechanisms, including precipitation of supersaturated phases (*7, 8*) and chemical perturbations that mobilize interstitial fines and coatings on framework grains (*9−11*).

Chemical perturbations must accomplish one or more of the following in order to mobilize these clay-size fines: (i) dissolution of a cementitious phase that mechanically binds or encapsulates the fines (2a → 3, 2b → 4 in Figure 1) (*4, 12, 13*); (ii) lysing of bonds among cross-bonded phases (1a → 3, 1b → 4 in Figure 1) (*14*); (iii) creation of like-charge on juxtaposed surfaces by altering the surface charge of variably
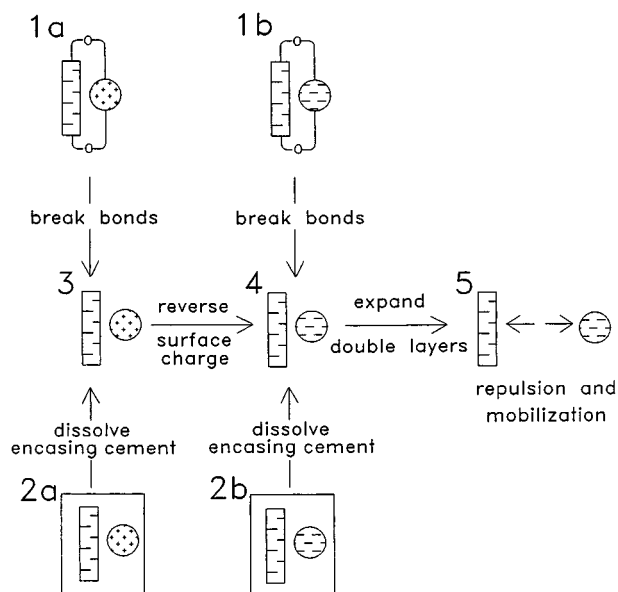
FIGURE 1. Schematic diagram of possible mechanistic sequences inducing colloid mobilization. For the Georgetown sediment, the circles represent amorphous iron oxyhydroxides and the plates represent clay minerals, predominantly kaolinite. Surface charge is represented. The squares encompassing the amorphous iron and kaolinite (states 2a,b) represent an amorphous silica cement mechanically binding or encapsulating these constituents. Bonds between the amorphous iron oxyhydroxides and kaolinite are represented in states 1a,b. Discrete goethite aggregates are not represented.

charged constituents (e.g., iron and aluminum oxides, kaolinite edges) through changes in pH or the addition of surface potential altering sorbates to pore fluids (3 → 4 in Figure 1) (*9, 10, 15*); and (iv) enhancement of electrostatic repulsion between juxtaposed surfaces of preexisting like-charge by lowering ionic strength (4 → 5 in Figure 1) (*16, 17*). It follows that the preexisting mineral associations dictate which sequence of chemical perturbations will mobilize colloids from a sediment.

As noted by Seaman et al. (*10*), few studies have examined colloid mobilization behavior in relatively undisturbed sediments. In addition, a systematic characterization of sediment structure must be coupled to studies of colloid release behavior if one is to elucidate the matrix constituents that play a key role in mobilization and if a broad understanding of the phenomenon is to be developed (*3*). To this end, we previously analyzed a Southeastern Coastal Plain aquifer sediment using analytical and transmission electron microscopy (AEM-TEM) to observe undisturbed associations among the inorganic matrix constituents and possible key binding agents (*18*). This AEM-TEM analysis indicated that an amorphous siliceous phase (approximately 10 wt % of the $<63\,\mu$m size fraction) appeared to mechanically cement (i.e., 2a,b in Figure 1) potentially mobilized matrix fines (e.g., kaolinite, goethite, quartz, and detectable amounts of vermiculite and gibbsite). In addition, a small amount (0.4 wt % of the $<63\,\mu$m size fraction) of amorphous iron oxyhydroxides was found to be distributed among and intimately associated with the clay minerals in the matrix. This observational evidence suggested that it is the amorphous iron oxyhydroxides that act as the effective electrostatic (3 in Figure 1) and/or bonding intermediary (1a,b in Figure 1) among kaolinite, which makes up approximately 45 wt %

* Corresponding author e-mail: pmgschwe@mit.edu; fax: 617-253-7395; phone: 617-253-1638.

of the <2 μm size fraction (*18*). It is improbable that this small amount of amorphous iron could encapsulate matrix fines. Goethite, although constituting approximately 95% of free iron in the sediment (10 wt % of the <63 μm size fraction), occurred as discrete aggregates within the matrix (*18*).

The objective of the current study was to ascertain whether the associations between the amorphous iron oxyhydroxides, amorphous silica, and clay minerals (i) are predominantly electrostatic in nature (3,4 in Figure 1) or (ii) respond only to stronger perturbations that lyse bonds (1a → 3, 1b → 4 in Figure 1) or dissolve cements (i.e., amorphous silica) potentially encapsulating the fines (2a → 3, 2b → 4 in Figure 1). We subjected columns packed with the same relatively undisturbed sediment previously characterized by AEM-TEM (*18*) to appropriate perturbing solutions to test these possibilities. The dissolved and colloidal elemental compositions of the column effluents were used to interpret mechanisms inducing mobilization and to differentiate various populations of matrix fines being mobilized.

Experimental Section

Sediment Characterization. The sediment is a 100 000-yr-old marine beach deposit (approximately 95% quartz) that constitutes a shallow, approximately 3 m thick, coastal plain aquifer located at the Belle Baruch Forest Sciences Institute, Georgetown, SC (*19*). The <63 μm and <2 μm size fractions represent 12% and 2.5 wt %, respectively, of this sediment (*18*). Organic carbon content is only 0.1 wt % of the bulk sediment (*20*). Groundwater pH is typically 5.2–5.3, conductivity is 38 ± 5 μS cm^{-1}, and ionic strength is 0.4 mM calculated using the major ions present in the groundwater (*18, 21*). Dissolved Fe, Al, and Si are 130 ± 100 nM, 170 ± 120 nM, and 370 ± 120 μM, respectively (*21*).

Sediment samples used for this study were obtained from the C horizon at a depth of 2.2 m during two coring events in June 1993 and March 1997. The coring locations were separated by approximately 0.3 m. Coring was accomplished using either a hollow stem auger (1993) or a hand auger (1997). The sample collected in 1993 was also used in the AEM-TEM analysis (*18*). During both sampling events, the approximately 5 kg field-moist samples were stored in sealed plastic bags and refrigerated for later use.

Column Apparatus and Experimental Procedures. A column apparatus used in a previous study of colloid mobilization (*9*) was modified slightly (see ref *21* for details). Argon was used to force prepared solutions from a pressure vessel (Millipore) to a 44 mm diameter filter cartridge containing approximately 5 g of moist sediment packed using a spatula within a 40 mm diameter O-ring. PTFE tubing was used for all connections. The void volume was determined to be approximately 1 mL. Effluent turbidity (Hach Ratio X/R) and pH (Radiometer) were monitored in-line downstream and recorded with a chart recorder. The turbidimeter was calibrated in-line with formazin standards. A valve placed upstream of the column maintained flow rates at 0.35–0.40 mL min^{-1} or seepage velocities of approximately 1.5 m d^{-1} assuming a porosity of 0.30.

A column containing no sediment was used to record initial pH and baseline turbidity measurements (typically ≤ 0.09 NTU) of the prepared solutions and to collect samples for determining background levels of dissolved Fe, Al, and Si for each experiment. The column was then isolated from upstream and downstream connections via stop valves, removed, and replaced with an identical column packed with sediment. The packed column was saturated via ascending flow and then reattached to the downstream portion of the apparatus. This procedure allowed the initial sediment response to be recorded with very minimal interference from any trapped air passing through the turbidity and pH flow cells. Column effluent was collected downstream in 2 mL microcentrifuge tubes. When a deionized water flush followed the initial solution treatment, flow was shut off at the upstream end of the column. Flow was restarted after the solutions were exchanged in the pressure vessel. This procedure took only 1–1.5 min. Slight jostling of the column caused by turning the stopcock on and off often resulted in a short turbidity spike lasting 1–2 pore volumes after flow was restarted. Turbidity returned to near-baseline levels before the effect of the deionized water was manifest in the turbidity profiles (4–5 pore volumes after flow recommenced).

Reagent grade L-ascorbic acid, oxalic acid, ammonium oxalate, and sodium phosphate monobasic (NaH$_2$PO$_4$) were used with deionized water (Vaponics) to prepare solutions. Anionic surfactant solutions were prepared with ultrapure sodium dodecyl sulfate (SDS) (GibcoBRL) and contained 40 μM HgCl$_2$ to inhibit biodegradation. Solution pH was modified with dilute HCl or NaOH solutions. A buffer, 0.2 mM sodium borate (Na$_2$B$_4$O$_7$), was used to help maintain elevated pH in some experiments (pH 8.0 and pH 8.8). All chemical treatments were performed in at least duplicate with fresh sediment.

Sample Analysis. Column effluent samples (2 mL each) were centrifuged at 23000g for 20 min. A 1-mL aliquot of each sample was then passed through a 30-nm pore-size polycarbonate filter (Osmonics). Dissolved Fe, Al, and Si were quantified using a 4100Zl graphite furnace atomic absorption (AA) spectrometer (Perkin-Elmer) calibrated with atomic absorption grade standards (Fisher) prepared in matrixes as close to sample compositions as possible. Effluent samples containing colloids were sonicated (81 W) for 1 h prior to the addition of 50 μL of 1.5 M HF to 1 mL of each sample. The samples were then shaken for 72 h before measuring the Fe and Al content of the digested samples by AA.

Electrophoretic Mobility Measurements. Electrophoretic mobility measurements were performed on model goethite colloids to approximate the effects of adsorption of the solutes investigated in the column experiments on the surface potentials of the iron oxyhydroxides present in the Georgetown sediment. We recognize that goethite and amorphous iron oxyhydroxides in the sediment may have differing surface properties which control the surface charge alterations that particular sorbates may impart on these solids. Goethite was synthesized (*22*), dialyzed against deionized water to remove excess ions, and stored in suspension for later use. X-ray diffraction (Rigaku 300) verified the existence of goethite in the suspension. The surface area of the air-dried goethite (22 m^2 g^{-1}) was obtained using nitrogen BET adsorption (Porous Materials, Ithaca NY). For each measurement, a given volume of the goethite suspension was added to the appropriate solution that had been made up in deionized water and brought to a specific pH using dilute NaOH or HCl solutions. The final solids' concentrations of these suspensions were approximately 75 mg L^{-1}, and the average particle size of the colloids in these suspensions was 350 ± 110 nm, as measured by laser light scattering (Coulter model N4). NaCl was also added to some solutions so that all solutions studied possessed ionic strengths in the range of 5–20 mM. Electrophoretic mobilities were measured with a Mark II microelectrophoresis apparatus (Rank Brothers, Bottisham, England) equipped with a 3 mW He/Ne laser. An average electrophoretic mobility for each solution condition was determined from measurement of 15–20 particles at both stationary levels (mobilities at each level were found to be equal).
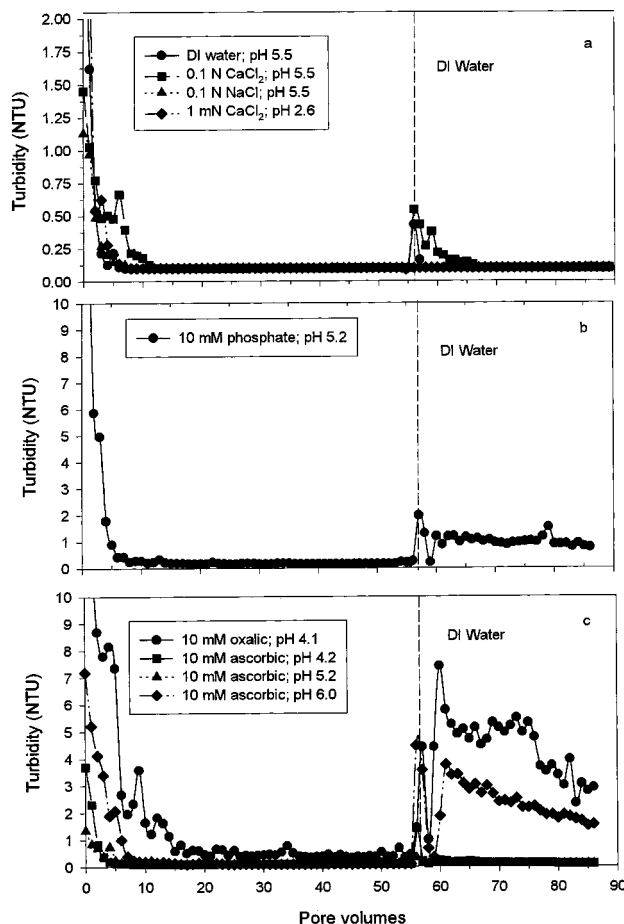
FIGURE 2. Turbidity profiles for sediment treated with (a) 0.1 N CaCl$_2$, 0.1 N NaCl, deionized water at pH 5.5, or 1 mN CaCl$_2$, pH 2.6; (b) 10 mM phosphate, pH 5.2; and (c) 10 mM oxalic acid, pH 4.1, and 10 mM ascorbic acid, pH 4.2, 5.2, and 6.0.

Results and Discussion

Effect of Ionic Strength. The relatively low ambient ionic strength (approximately 0.4 mM) and low turbidity (<0.1 NTU) of the groundwater at the site indicated that this sediment would not respond to perturbations causing electric double-layer expansion (4 → 5 in Figure 1). Indeed, turbidity remained close to background levels (≤0.09 NTU) when high ionic strength solutions (0.1 N NaCl and 0.1 N CaCl$_2$ at pH 5.5) were exchanged for deionized water in the packed-column experiments (Figure 2a). Only the deionized water flush following the 0.1 N CaCl$_2$ treatment resulted in slightly elevated and briefly sustained turbidity levels (to approximately 0.18 NTU) upon contact of the sediment with the deionized water (approximately pore volumes 60–65 in Figure 2a). The turbidity spikes centered at pore volume 56 (Figure 2a) for both experiments were due to column movement during the solution exchange procedure. Turbidity manifest at the beginning of 0.1 N NaCl, 0.1 N CaCl$_2$, and deionized water treatments (1.0–3.0 NTU, pore volumes 1–10, Figure 2a) was assumed to be due to the release of loose material resulting from column packing; turbidity fell to background levels within approximately 5 pore volumes after initiation of the treatment flushes. Length of contact time with the salt solutions was not a factor, as experiments were replicated to as many as 150 pore volumes before following with a deionized water flush.

As only juxtaposed like-charged constituents would be repulsed by double-layer expansion, these results imply that (a) surface charge repulsion among the negatively charged faces of the abundant kaolinite booklets was mitigated by
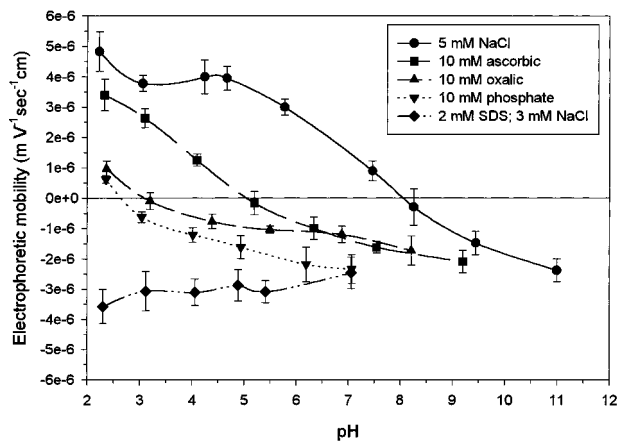

FIGURE 3. Electrophoretic mobilities of model goethite colloids in equilibrium with various solutions used as treatment solutions in the column experiments. Error bars represent ± 1σ.

positively charged amorphous iron oxyhydroxides distributed among them (i.e., 3 in Figure 1) (18) and/or (b) the amorphous iron oxyhydroxide or amorphous silica phase chemically or mechanically bound the matrix (1a,b or 2a,b, respectively, Figure 1) so that repulsive forces among these constituents could not induce mobilization. These results also suggested that the goethite aggregates, composed of intimately associated 5–10 nm spheroids with presumably similar surface charge (analogous to 4 in Figure 1) (18), were (i) positively charged and surrounded by negatively charged surfaces (e.g., kaolinite faces) and (ii) the spheroids acted in aggregate, i.e., the spheroids were not repelled from each other, due possibly to sintering by amorphous iron.

Effect of Treatment with Phosphate and Surfactant. If both the amorphous iron oxyhydroxide intermediaries among the kaolinite faces and the goethite aggregates were positively charged under native groundwater conditions, reversing their surface charge and then lowering ionic strength may induce colloid release (i.e., 3 → 4 → 5 in Figure 1). To this end, we treated the sediment with 2 mM SDS at pH 5.4 and 10 mM phosphate at pH 5.2 to impart negative charge to the iron oxyhydroxides (23, 24). At pH 5.2–5.4, both 2 mM SDS and 10 mM phosphate reversed the surface charge of model goethite colloids, which had a pH$_{pzc}$ (pH at the point of zero charge) of approximately 8.0 in 5 mM NaCl (Figure 3), a value within the range of 7.0–9.7 observed by others (25, 26). The pH$_{pzc}$ of naturally occurring goethite and amorphous iron oxyhydroxides would be expected to be lower (27).

The sediment showed no response during treatment with the 2 mM SDS solution for up to 100 pore volumes (the duration required to attain effluent SDS concentrations within 1–2% of the influent concentration (21)) or during the deionized water flush that followed (data not shown). Colloids were mobilized in the deionized water flush following the 10 mM phosphate treatment (Figure 2b). This mobilization peaked at approximately 1 NTU and slowly declined within the 30 pore volume deionized water flush (Figure 2b). The average Al/Fe mole ratio of these colloids (0.5 ± 0.3, Table 1) was more iron-rich than the bulk matrix (3.2 ± 0.2, Table 1). The comparatively lower Al/Fe ratio of these colloids suggests that goethite aggregates (Al/Fe mole ratio of 0.24 ± 0.08 (18)) may have been mobilized preferentially by the phosphate/deionized water treatment. Recently, Seaman et al. (28) observed preferential mobilization of goethite in a mineralogically similar coastal plain sediment, which supports the inferences made from our observations. In the Georgetown sediment, the goethite aggregates apparently were more free to respond (i.e., be mobilized) to repulsive interactions generated by treatment of the sediment with

TABLE 1. Dissolved Fe in Treatment Solution Effluents and Al/Fe Mole Ratios of Mobilized Colloids

treatment	dissolved Fe in treatment solution effluent (nmol min^{-1})	% Fe dissolved during treatment flush as fraction of total amorphous Fe[a]	Al/Fe mole ratio of colloids mobilized[b]
DI water; pH 5.5	ND[c]	ND	NR[d]
0.1 N CaCl$_2$; pH 5.5	ND	ND	NR
0.1 N NaCl; pH 5.5	ND	ND	NR
2 mM SDS, 1 mM NaCl; pH 5.4	ND	ND	NR
10 mM phosphate; pH 5.2	ND	ND	0.5 ± 0.3 ($n = 22$)[e]
10 mM oxalic; pH 4.1	9.0 ± 0.5 ($n = 34$)	2.9	3.1 ± 0.7 ($n = 19$)[e]
10 mM ascorbic; pH 4.2	3.6 ± 0.3 ($n = 51$)	1.2	NR
10 mM ascorbic; pH 5.2	1.4 ± 0.1 ($n = 34$)	0.5	NR
10 mM ascorbic; pH 6.0	0.7 ± 0.1 ($n = 51$)	0.2	2.5 ± 1.4 ($n = 9$)[e]
0.2 mM Na$_2$B$_4$O$_7$; pH 8.8	ND	ND	1.5 ± 0.5 ($n = 11$)[e]
1 mM CaCl$_2$; pH 2.6	0.16 ± 0.03 ($n = 24$)	0.05	NR
1 mM phosphate; pH 5.2	ND	ND	NR
1 mM ascorbic; pH 5.2	0.15 ± 0.01 ($n = 19$)	0.05	NR
0.5 mM ascorbic + 0.5 mM phosphate; pH 5.2	0.06 ± 0.02 ($n = 14$)	0.02	2.3 ± 0.9 ($n = 23$)[f]

[a] Based on integration of dissolved Fe in 50 pore volumes of treatment effluent divided by total amorphous Fe present in column. Total amorphous Fe present was calculated using 64 μmol amorphous Fe g^{-1} <63 μm size fraction determined using the ammonium oxalate method (22). [b] Compare to Al/Fe mole ratio of bulk matrix 3.2 ± 0.2 (measured from digestion of <63 μm size fraction (22)). [c] ND, not detected (≤1 ppb) or indifferentiable from background levels. [d] NR, no colloids released. [e] Al/Fe mole ratio for colloids released during deionized water flush following treatment flush. [f] Al/Fe mole ratio for colloids released during the treatment flush.

phosphate than were the rest of the bulk matrix constituents, particularly the abundant kaolinite books and associated amorphous iron oxyhydroxides (18). These data further suggest that (i) amorphous silica mechanically binding the kaolinite books (i.e., in 1a → 3,1b → 4 in Figure 1) or (2) cross-bonding between the amorphous iron oxyhydroxides and kaolinite (i.e., 2a → 3, 2b → 4 in Figure 1) hindered repulsive electrostatic interactions from inducing mobilization of these phases.

Effect of Treatment with Organic Acids. To break potential bonds between the amorphous iron oxyhydroxides and kaolinite (1a → 3 in Figure 1), we treated the sediment with the reductant, l-ascorbic acid, and a complexant (in the absence of light), oxalic acid (29, 30). Treatment of the sediment with oxalic acid at pH 4.1 resulted in an extended initial release of colloids to 15 pore volumes as well as continued release at approximately 0.5–1.0 NTU (Figure 2c) over the 56 pore volume duration of the treatment. During the deionized water flush that followed, turbidity peaked initially at approximately 8 NTU and then leveled off at 5–6 NTU (pore volumes 65–75, Figure 2c) before gradually declining. During treatment with ascorbic acid at pH 4.2, 5.2, and 6.0, no sustained turbidity was observed after the initial release, although the initial pulse during the pH 6.0 ascorbic acid treatment was notably larger than during the pH 4.2 and pH 5.2 treatments (Figure 2c). Sustained turbidity was observed only during the deionized water flush that followed the pH 6.0 ascorbic acid treatment (Figure 2c). This pulse peaked at approximately 4 NTU and declined similarly as that which occurred during the deionized water flush that followed the pH 4.1 oxalic acid treatment.

The Al/Fe mole ratios of the colloids released in the deionized water flushes following the oxalic acid (3.1 ± 0.7, Table 1) and pH 6.0 ascorbic acid (2.5 ± 1.4, Table 1) treatments differed greatly from those released by the 10 mM phosphate treatments (0.5 ± 0.3, Table 1). Apparently, the oxalic acid and pH 6.0 ascorbic acid treatments promoted mobilization of fines more similar in bulk composition to the entire bulk matrix (3.2 ± 0.2, Table 1). To convert turbidity from NTU units to mg of colloidal solid L^{-1}, we employed a relation obtained using kaolin standards (9). When the Fe (μM) concentrations in the digests for each of these samples were regressed against the turbidities of the samples (in g of colloidal solids L^{-1}), a slope of 1400 μmol g^{-1} colloidal solid ($R^2 = 0.85$) was obtained. This value corresponds well to

the amount of Fe measured in the bulk matrix (1360 ± 95 μmol g^{-1} <63 μm size fraction (18)), suggesting that 1 g of colloidal solid corresponded to 1 g of <63 μm size fraction. This supports our contention that these Al/Fe mole ratios indicate colloids representative of the entire bulk matrix were mobilized after treatment with pH 6.0 ascorbic acid and pH 4.1 oxalic acid.

Lysing of bonds among amorphous iron oxyhydroxides and clay minerals, concomitant with dissolution of the iron oxyhydroxides in the sediment, may explain why the oxalic acid and pH 6.0 ascorbic acid treatments appear to have mobilized colloids representative of the entire bulk matrix. It is improbable that dissolution induced mobilization by altering existing juxtapositions from clay mineral–iron oxide–clay mineral to more repulsive clay mineral–clay mineral (9) associations during our experiments. Note that the integrated amounts of Fe released in any of these organic acid treatments represented only a very small percentage of the total amorphous Fe present (Table 1), even if one assumes that all of the dissolved Fe was derived from the amorphous iron oxyhydroxides and not from the goethite as well.

The pH-dependent colloid release behavior observed for the ascorbic acid treatments suggested that, although lysis of bonds among the amorphous iron oxyhydroxides and clay minerals appeared to be necessary for mobilization of the bulk matrix, this effect alone was not sufficient to induce mobilization (i.e., 1b → 4 in Figure 1 is not viable). Concomitantly, sufficient negative charge had to be imparted to the amorphous iron oxyhydroxides before lowering ionic strength in order to induce mobilization of the bulk matrix (i.e., 1a → 3 → 4 → 5 in Figure 1). Electrophoretic mobility data using model goethite colloids suspended in 10 mM ascorbic acid solutions explains qualitatively the pH-dependent mobilization behavior observed for the sediment when treated with 10 mM ascorbic acid. When suspended in 10 mM ascorbic acid, the pH$_{pzc}$ of the goethite colloids was shifted from approximately pH 8.0 (5 mM NaCl) to approximately pH 5.0 (Figure 3). Apparently, the pH at which specifically adsorbed ascorbic acid was able to reverse the surface charge of the amorphous iron oxyhydroxide intermediaries in the sediment lay between pH 4 and pH 6 as well, as mobilization of the bulk matrix was observed only after treatment with 10 mM ascorbic acid at pH 6, with no release at all observed at pH 4 or pH 5.2 (Figure 2c). Note that the pH$_{pzc}$ of the goethite colloids was shifted to an even
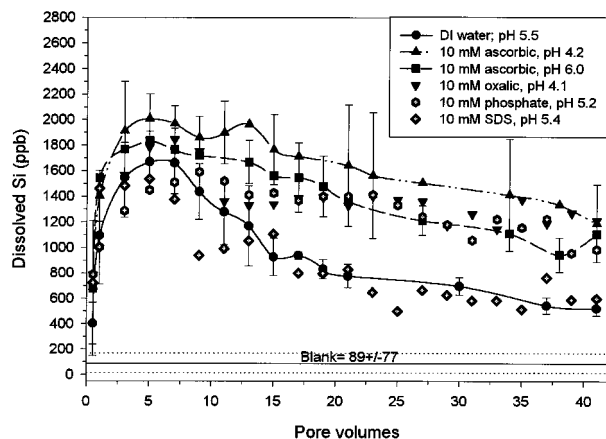
FIGURE 4. Profiles of dissolved Si (ppb) measured in treatment solutions eluting from columns. Use of error bars ($\pm 1\sigma$) alternates between samples for the 10 mM ascorbic acid pH 4.2 and pH 6.0 treatments ($n = 3$) to avoid overlap; $n = 5$ for the deionized water (DI) treatments. The oxalic acid, phosphate, and SDS data represent single sample measurements.

lower value (pH 3) in solutions containing 10 mM oxalic acid (Figure 3). Correspondingly, 10 mM oxalic acid was able to induce mobilization of the bulk matrix at a lower pH (pH 4.1, Figure 2c) than was ascorbic acid. The ability of oxalate to impart greater repulsive forces than ascorbate through specific adsorption correlates with the lower aqueous acidity constants ($pK_1 = 1.5$ and $pK_2 = 4.2$ (31)) of oxalic acid as compared to those of ascorbic acid ($pK_1 = 4.28$, $pK_2 = 11.5$ (31)).

Dissolution of an encapsulating amorphous silica cement did not appear to be required to induce mobilization of the bulk matrix. If it were necessary, one would have expected higher dissolved Si levels in the effluent during the ascorbic and oxalic acid treatments than during the phosphate treatment. However, dissolved Si in the effluent from the oxalic and ascorbic acid treatments and phosphate treatment were indistinguishable from each other, suggesting that the amorphous silica played little, if any, role in mechanically binding the matrix (Figure 4). Note, though, that dissolved Si levels in the effluent from the oxalic and ascorbic acid and phosphate treatments were elevated above the levels measured in effluent from treatments containing only deionized water or SDS (Figure 4). The elevated levels of dissolved Si in the oxalic acid, ascorbic acid, and phosphate treatments probably represent ambiently adsorbed silicate that was more readily displaced from solid surfaces by oxalate, ascorbate, and phosphate ligands than by deionized water or SDS (32). That SDS was not able to displace adsorbed silicate may indicate that SDS adsorption and admicelle formation were hindered by ambiently adsorbed ligands. This may explain why no iron-rich colloids were mobilized during treatment with the surfactant in contrast to the phosphate treatment.

Effect of Elevated pH. When treated with a pH 8.0 solution, only limited, sporadic release above a value of 0.5 NTU occurred (Figure 5a). At pH 8.8, sustained colloid mobilization began only after approximately 80 pore volumes and grew to values of several NTU by 190 pore volumes (Figure 5a). The average Al/Fe mole ratio of these colloids (1.5 ± 0.5, Table 1), although half that determined for the bulk matrix (3.2 ± 0.2, Table 1), was much higher than that determined for the colloids released during the deionized water flush following the 10 mM phosphate treatment (0.5 ± 0.3, Table 1).

The higher Al/Fe mole ratio of the colloids mobilized by the pH 8.8 treatment, relative to those mobilized by the phosphate/deionized water treatment, may indicate that the former induced mobilization of colloids more representative
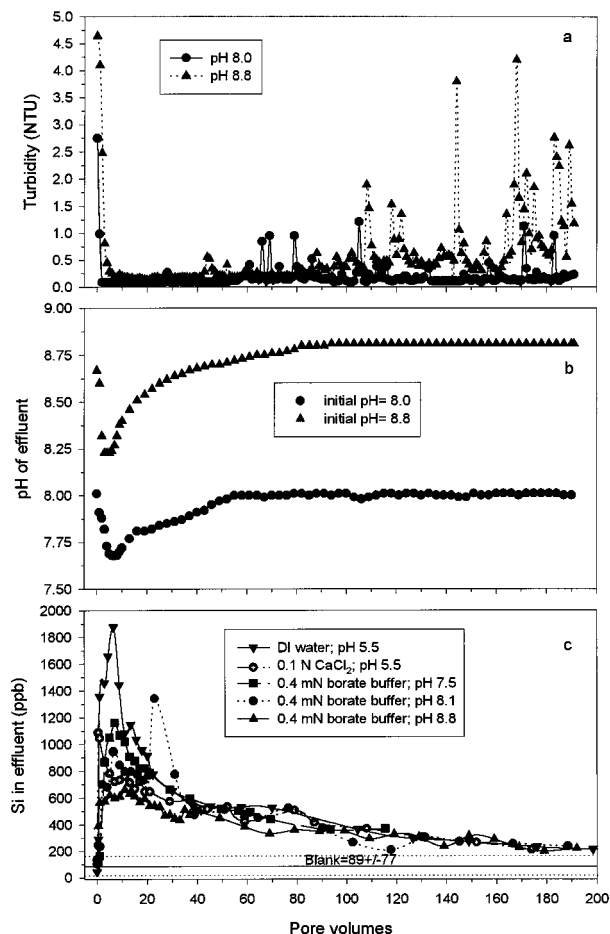

FIGURE 5. (a) Turbidity profiles for experiments in which sediment was subjected to pH 8.0 and pH 8.8 solutions. (b) pH profiles for the elevated pH treatments. Note the initially lower pH of the effluents for both experiments and the gradual rise to the influent pH. (c) Profiles of dissolved Si (ppb) measured in the effluents from columns subjected to treatment solutions at various pH and ionic strength values.

of the entire bulk matrix (e.g., more kaolinite). The electrophoretic mobilities of model goethite colloids indicated that 10 mM phosphate at pH 5.2 and a pH 8.8 solution would be similarly capable of imparting negative charge to amorphous iron oxyhydroxide surfaces in the sediment (Figure 3). Thus, although delayed mobilization coincided approximately with a rise in effluent pH after initial titration by the sediment (Figure 5b), the mobilization event does not appear to have been caused merely by surpassing the pH_{pzc} of the iron oxyhydroxides in the sediment. Dissolved Si levels in the pH 8.8 treatment were indistinguishable from dissolved Si levels in treatments at lower pH (Figure 5c), indicating that dissolution of amorphous silica was not playing a role in colloid mobilization during the elevated pH treatment either. Rather, it appears that sustained release was delayed in this experiment until pore fluid pH attained high enough values (Figure 5c) to (i) sufficiently *hydrolyze* bonds among the amorphous iron oxyhydroxides and kaolinite (no dissolution appeared to have occurred in the pH 8.8 experiment, as dissolved Fe was not detectable (≤ 1 ppb, Table 1)) and (ii) reverse the surface charge of the amorphous iron oxyhydroxides as well as the surface charge of the goethite aggregates. Apparently, phosphate (or SDS) was not capable of hydrolyzing these bonds. Note that dissolved Fe was not detectable in effluent from the phosphate (or SDS) treatment either (Table 1).

Effect of Acidic pH. Acidic pH levels (<5) induced by cation exchange processes have been associated with colloid
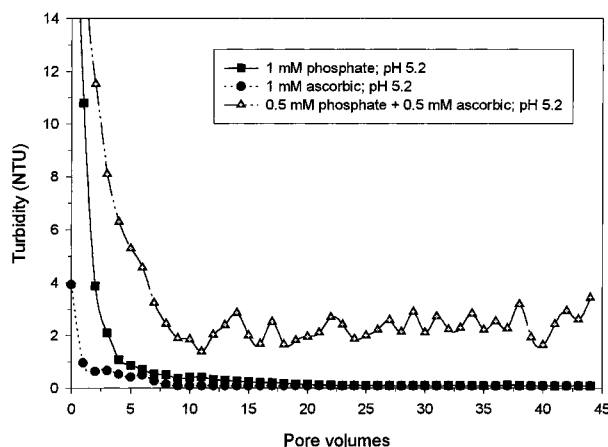
FIGURE 6. Turbidity profiles for effluent from columns subjected to 1 mM phosphate, 1 mM ascorbic acid, and a combination of 0.5 mM phosphate and 0.5 mM ascorbic acid, all at pH 5.2.

mobilization in other coastal plain sediments (*10*). In that study, enhancement of positive charge on variably charged constituents (e.g., iron oxides) by the acidic pH was thought to induce mobilization of positively charged colloids later identified as predominantly goethite (*28*). We treated the Georgetown sediment with 1 mN $CaCl_2$ at pH 2.6 for 56 (Figure 2a) and 150 pore volumes (data not shown) before flushing with deionized water. No response from the sediment was observed in either case.

The juxtaposition of positively charged amorphous iron oxyhydroxides with negatively charged kaolinite faces, associations that we believe predominate in the Georgetown sediment, would be expected to be attractive at acidic pH regardless of whether proton-promoted dissolution was lysing bonds among these two constituents (note that dissolved Fe was measurable in the pH 2.6 treatment effluent, Table 1). Therefore, one would not expect these constituents to be mobilized under these conditions, in agreement with our observations. That the goethite aggregates were not mobilized either suggested that (i) attractive forces created between the positively charged spheroids and surrounding negatively charged kaolinite faces were stronger than spheroid-spheroid repulsion or (ii) spheroid–spheroid repulsion was inhibited by the sintering together of the spheroids.

Mechanisms of Colloid Detachment. It appears that mobilization of colloids representative of the entire bulk matrix can occur when this sediment is subjected to a *combination* of solutes that (i) break bonds between amorphous iron oxyhydroxides and kaolinite via dissolution or hydrolysis mechanisms and (ii) impart sufficient negative charge to the amorphous iron oxyhydroxides to promote repulsive interactions with kaolinite faces. In addition, ionic strength must be low enough so that sufficiently thick double layers promote electrostatic repulsion that exceeds van der Waals attraction among neighboring phases. Sediment response to relatively low (1 mM) levels of ascorbic acid or phosphate at pH 5.2 supports this mechanism (Figure 6). Neither 1 mM ascorbic acid nor 1 mM phosphate treatments alone at pH 5.2 induced sustained mobilization of colloids (Figure 6). However, when 0.5 mM ascorbic and 0.5 mM phosphate were added together at pH 5.2, sustained release of colloids occurred at levels of 2–3 NTU over the 40 pore volume duration of the treatment. The Al/Fe mole ratio of the colloids was 2.3 ± 1.0 (Table 1), suggesting that mobilization of colloids fairly representative of the entire bulk matrix was occurring.

The mineralogical composition and structural associations existing in any sediment are dictated, in large part, by diagenetic processes. Recurrent oxidation and reduction

reactions and the presence of solutes that interfere with crystallization (*33, 34*) can promote amorphous or weakly crystalline phases that may become intimately associated with other sediment fines (e.g., clay minerals). Indeed, Golden and Dixon (*14*) found that mixtures of kaolinite and iron oxyhydroxides, formed by oxidation in the presence of the kaolinite, did not respond to electrostatic perturbations, whereas mechanical mixtures of these two constituents did. They hypothesized that bonds held the iron oxide−clay mineral aggregates intact, inhibiting electrostatic dispersion. As the results of our study imply, such associations may inhibit the effects of chemical perturbations that might substantially mobilize fines in older, more crystalline (and by inference, less cross-bonded) deposits. Recognition of such diagenetic differences among deposits is important in developing an understanding of the various mechanisms which generate colloids in the subsurface.

Acknowledgments

Literature Cited

(1) McCarthy, J. F.; Zachara, J. M. *Environ. Sci. Technol.* **1989**, *23*, 496−502.
(2) Puls, R. W.; Powell, R. M. *Environ. Sci. Technol.* **1992**, *26*, 614−621.
(3) Ryan, J. N.; Elimelech, M. *Colloids Surf. A* **1996**, *107*, 1−56.
(4) Ronen, D.; Margaritz, M.; Weber, U.; Amiel, A. J. *Water Resour. Res.* **1992**, *28*, 1279−1291.
(5) Ryan, J. N.; Gschwend, P. M. *Geochim. Cosmochim. Acta* **1992**, *56*, 1507−1521.
(6) Kaplan, D. I.; Bertsch, P. M.; Adriano, D. C.; Miller, W. P. *Environ. Sci. Technol.* **1993**, *27*, 1193−1200.
(7) Gschwend, P. M.; Reynolds, M. D. *J. Contam. Hydrol.* **1987**, *1*, 309−327.
(8) Liang, L.; McCarthy, J. C.; Jolley, L. W.; McNabb, J. A.; Mehlhorn, T. L. *Geochim. Cosmochim. Acta* **1993**, *57*, 1987−1999.
(9) Ryan, J. N.; Gschwend, P. M. *Environ. Sci. Technol.* **1994**, *28*, 1717−1726.
(10) Seaman, J. C.; Bertsch, P. M.; Miller, W. P. *Environ. Sci. Technol.* **1995**, *29*, 1808−1815.
(11) Kaplan, D. I.; Bertsch, P. M.; Adriano, D. C. *Groundwater* **1995**, *33*, 708−717.
(12) Gschwend, P. M.; Backhus, D. A.; MacFarlane, J. K.; Page, A. L. *J. Contam. Hydrol.* **1990**, *6*, 307−320.
(13) Ryan, J. N.; Gschwend, P. M. *Water Resour. Res.* **1990**, *26*, 307−322.
(14) Golden, D. C.; Dixon, J. B. *Soil Sci. Soc. Am. J.* **1985**, *49*, 1568−1576.
(15) Kia, S. F.; Fogler, H. S.; Reed, M. G. *J. Colloid Interface. Sci.* **1987**, *118*, 158−168.
(16) McDowell-Boyer, L. M. *Environ. Sci. Technol.* **1992**, *26*, 586−593.
(17) Roy, S. B.; Dzombak, D. *Colloids Surf.* **1996**, *107*, 245−262.
(18) Swartz, C. H.; Ulery, A. L.; Gschwend, P. M. *Geochim. Cosmochim. Acta* **1997**, *61*, 707−718.
(19) Williams, T. M.; McCarthy, J. F. Field-scale tests of colloid: facilitated transport. In *National Research and Development Conference on the Control of Hazardous Materials*; Hazardous Materials Control Research Institute: Anaheim, CA, 1991; pp 179−184.
(20) Holmén, B. A.; Gschwend, P. M. *Environ. Sci. Technol.* **1997**, *31*, 105−113.
(21) Swartz, C. H. Ph.D. Thesis, Massachusetts Institute of Technology, 1998.
(22) Atkinson, R. J.; Posner, A. M.; Quirk, J. P. *J. Inorg. Nucl. Chem.* **1968**, *30*, 2371−2381.
(23) Hansmann, D. D.; Anderson, M. A. *Environ. Sci. Technol.* **1985**, *19*, 544−551.
(24) Chandar, P.; Somasundaran, P.; Turro, N. J. *J. Colloid Interface. Sci.* **1987**, *117*, 31−46.

(25) Borgaard, O. K. *Clays Clay Miner.* **1983**, *31*, 230−232.

(26) Zeltner, W. A.; Anderson, M. A. *Langmuir* **1988**, *4*, 469−474.

(27) Schwertmann, U.; Fechter, H. *Clay Miner.* **1982**, *17*, 471−476.

(28) Seaman, J. C.; Bertsch, P. M.; Strom, R. N. *Environ. Sci. Technol.* **1997**, *31*, 2782−2790.

(29) Zinder, B.; Furrer, G.; Stumm, W. *Geochim. Cosmochim. Acta* **1986**, *50*, 1861−1869.

(30) Suter, D.; Banwart, S.; Stumm, W. *Langmuir* **1991**, *7*, 809−813.

(31) *The Merck Index*, 12th ed.; Budavari, S., Ed.; Merck and Co., Inc.: Whitehouse Station, NJ, 1996.

(32) Torrent, J.; Schwertmann, U.; Barron, V. *Clays Clay Miner.* **1992**, *40*, 14−21.

(33) Cornell, R. M.; Schwertmann, U. *Clays Clay Miner.* **1979**, *27*, 402−410.

(34) Anderson, P. R.; Benjamin, M. M. *Environ. Sci. Technol.* **1985**, *19*, 1048−1053.